Published in final edited form as:
J Neurochem. 2009 June ; 109(5): 1225–1236. doi:10.1111/j.1471-4159.2009.06037.x.

Cellular calcium deficiency plays a role in neuronal death caused by proteasome inhibitors

Shengzhou Wu[1,2], **Krzysztof L. Hyrc**[1,2], **Krista L. Moulder**[1,3], **Ying Lin**[1,2], **Timothy Warmke**[1,2], and **B. Joy Snider**[1,2]

[1]laboratory of B. Joy Snider, Hope Center for Neurological Disorders, Washington University School of Medicine, Saint Louis, MO, USA

[2]laboratory of B. Joy Snider, Department of Neurology, Washington University School of Medicine, Saint Louis, MO, USA

[3]laboratory of B. Joy Snider, Department of Psychiatry, Washington University School of Medicine, Saint Louis, MO, USA

Abstract

Cytosolic Ca^{2+} concentration ($[Ca^{2+}]_i$) is reduced in cultured neurons undergoing neuronal death caused by inhibitors of the ubiquitin proteasome system. Activation of calcium entry via voltage-gated Ca^{2+} channels restores cytosolic Ca^{2+} levels and reduces this neuronal death (Snider et al. 2002). We now show that this reduction in $[Ca^{2+}]_i$ is transient and occurs early in the cell death process, before activation of caspase-3. Agents that increase Ca^{2+} influx such as activation of voltage-gated Ca^{2+} channels or stimulation of Ca^{2+} entry via the plasma membrane Na-Ca exchanger attenuate neuronal death only if applied early in the cell death process. Cultures treated with proteasome inhibitors had reduced current density for voltage-gated Ca^{2+} channels and a less robust increase in $[Ca^{2+}]_i$ after depolarization. Levels of endoplasmic reticulum (ER) Ca^{2+} were reduced and capacitative Ca^{2+} entry was impaired early in the cell death process. Mitochondrial Ca^{2+} was slightly increased. Preventing the transfer of Ca^{2+} from mitochondria to cytosol increased neuronal vulnerability to this death while blockade of mitochondrial Ca^{2+} uptake via the uniporter had no effect. Programmed cell death induced by proteasome inhibition may be caused in part by an early reduction in cytosolic and endoplasmic reticulum (ER) Ca^{2+}, possibly mediated by dysfunction of voltage-gated Ca^{2+} channels. These findings may have implications for the treatment of disorders associated with protein misfolding in which proteasome impairment and programmed cell death may occur.

Keywords

endoplasmic reticulum; mitochondria; calcium imaging; caspase; capacitative calcium entry

Inhibition of the ubiquitin proteasome system (UPS) causes programmed cell death in many cell types, including neurons. We hypothesized that the neuronal death caused by proteasome inhibition might be associated with dysregulation of calcium (Ca^{2+}) homeostasis, specifically with a reduction, rather than an increase, in neuronal Ca^{2+}. Many studies have focused on increases in intracellular Ca^{2+} in disorders including stroke, epilepsy, trauma and neurodegenerative disorders (for recent reviews see Arundine and Tymianski 2004; Berliocchi et al. 2005). The role of reductions in intracellular Ca^{2+} in

Corresponding author: Dr. B. Joy Snider Hope Center for Neurological Disorders Department of Neurology, Washington University School of Medicine Campus Box 8111 660 S. Euclid Saint Louis, MO 63110 Email: sniderj@neuro.wustl.edu .

neuronal death has also been studied, primarily in developing neurons, and a "calcium set point" has been hypothesized to play a key role in neuronal survival (Johnson et al. 1992). We have previously reported that free cytosolic Ca^{2+} ($[Ca^{2+}]_i$) is reduced in cultured murine neocortical neurons after 1-4 hr treatment with proteasome inhibitors. We observed a similar reduction in $[Ca^{2+}]_i$ in cultures treated with staurosporine, a protein kinase inhibitor that causes neuronal death associated with activation of programmed cell death pathways (Snider et al. 2002; Canzoniero et al. 2004). However, other investigators have reported that treatment with proteasome inhibitors increases $[Ca^{2+}]_i$ (Landowski et al. 2005; Lee et al. 2005; Nawrocki et al. 2005b; Nawrocki et al. 2005a). These apparently conflicting results could represent differences in cell type, intensity of injury or timing of assessment of $[Ca^{2+}]_i$ relative to injury. For example, there could be an early increase and subsequent decline in $[Ca^{2+}]_i$ levels, or Ca^{2+} could be reduced in some cellular compartments and increased in others, as reported in cultured mesencephalic neurons treated with ceramide (Darios et al. 2005). Understanding the nature and timing of these derangements in Ca^{2+} homeostasis might have significant implications for designing rational treatment strategies for conditions where neuronal proteasome activity is impaired. We hypothesized that the neuronal death associated with impairment of the UPS was caused in part by transfer of Ca^{2+} between cytosol, ER and mitochondria and set out to clarify the timing of changes in $[Ca^{2+}]_i$ relative to cell death and to identify mechanisms responsible for the alterations in $[Ca^{2+}]_i$ and neuronal death under these conditions. A preliminary report of these studies has appeared in abstract form (Wu et al. 2006).

Materials and Methods

Preparation of murine neocortical cultures

Mixed neocortical cultures containing both neurons and astrocytes were prepared from mouse cortices as previously described (Rose et al. 1993; Lee et al. 2004). Briefly, dissociated neocortices obtained from fetal Swiss-Webster mice at 14-16 days gestation were plated onto a previously established glial monolayer. Unless otherwise indicated, experiments were performed on cultures after 13-14 days in vitro. Near-pure neuronal cultures were prepared by plating neocortices directly onto culture vessels that had been coated with poly-D-lysine (100 μg/ml) and laminin (4 μg/ml) prior to plating. These cultures contain less than 5% astrocytes; experiments on these cultures were performed 7-8 days after plating.

Calcium imaging

Measurements of $[Ca^{2+}]_i$ were performed using fura-2 video microfluorimetry as previously reported (Snider et al. 2002; Canzoniero et al. 2004). All washes and imaging were carried out in HEPES buffered saline (144 mM NaCl, 10 mM glucose, 10 mM HEPES, 5 mM KCl, 1.8 mM $CaCl_2$, 1 mM $MgCl_2$, 10 μM glycine, pH = 7.2) in room air unless otherwise indicated. Cells were incubated for 45 min at room temperature with 5 μM fura-2 AM (Invitrogen, Carlsbad, CA), and incubated in buffer without fura-2 for another 30 min. Cultures treated with proteasome inhibitors and other compounds were processed in parallel with sham washed (treated with vehicle only) cultures. Cultures were imaged with a Nikon Eclipse TE300 inverted microscope (Nikon Instruments, Melville, NY) using UV illumination via a monochrometer (Till Photonics Polychrome II) and a 40X oil immersion objective, fitted with a 12 bit SensiCam CCD camera (Cooke Corp., Tonawanda, NY). Excitation wavelengths were alternated between 340 and 380 nm, and emissions were measured at ≥ 510 nm. Because neuronal cell bodies sit well above the underlying glial monolayer, it was possible to detect the 340/380 fluorescence originating in these cell bodies with minimal interference from underlying glia. This data is presented as excitation ratios in the figures. For comparison, in text we provide the $[Ca^{2+}]_i$ estimated by translating

fluorescence ratios (340/380 nm) to $[Ca^{2+}]_i$ using the method of Grynkiewicz et al. (Grynkiewicz et al. 1985). Briefly, the calcium concentrations were determined by the formula:

$$\left[Ca^{2+}\right]_i = K_d \quad Q\,(R - R_{min}) / (R_{max} - R)$$

Where K_d is the fura-2 apparent dissociation constant for calcium, Q is the ratio of F_{min} to F_{max} at 380 nm and R is the ratio of fluorescence intensity excited at 340 and 380 nm at the given time point during the experiment. The calibration values were determined *in situ* in the presence of 1.8 mM free Ca^{2+} (R_{max}) or 2 mM EGTA (R_{min}) with the co-application of 4 μM ionomycin.

$[Ca^{2+}]_{mito}$ was measured similarly, except that cultures were washed, prior to imaging, with buffer lacking Ca^{2+} and containing ethylene glycol-bis(2-aminoethylether)-N,N,N,N'-tetraacetic acid (EGTA, 50 μM). Images were captured before and after application of the mitochondrial uncoupling agent protonophore carbonylcyanide-p-trifluoromethoxy-phenylhydrazone (FCCP, 10 μM for 10 min) as a measure of Ca^{2+} released from depolarized mitochondria, similar to the methods described by Brocard et al. (2001) and Thayer and Miller (1990).

$[Ca^{2+}]_{ER}$ was measured as described by (Darios et al. 2005) using mag-fura-2 (furaptra). Mag-fura-2 has relatively low affinity for Ca^{2+} (K_d reported between 25-100 μM, Raju et al. 1989; Ravin et al. 1997) and tends to accumulate in intracellular compartments, making it useful for measurement of $[Ca^{2+}]_{ER}$ (Solovyova et al. 2002). Cultures were loaded with mag-fura-2 (10 uM) and Pluronic F-127 (0.05%) for 1 hr at 37 °C in buffer containing 125 mM NaCl, 5 mM KCl, 1 mM $MgSO_4$, 1mM Na_2HPO_4, 5.5 mM glucose, 20 mM $NaHCO_3$, 2 mM L-glutamine, and 20 mM HEPES, pH 7.2. The cells were washed and kept in dye-free media for 1 hr prior to imaging. Images were obtained as described above for fura-2. In our experiments, mag fura-2 K_d for Ca^{2+} as determined by *in situ* calibration was 184 μM, somewhat higher than reported values.

In some experiments, $[Ca^{2+}]_{ER}$ was also measured indirectly. Prior to imaging, cultures were washed with buffer lacking Ca^{2+} and containing EGTA (50 μM). Images were captured before and after application of the thapsigargin (5 μM) to block ER Ca^{2+} uptake. After 5 min, Ca^{2+} was added to the extracellular bathing media and images were captured for an additional 5 min.

Electrophysiology

Whole-cell recordings were performed using an Axopatch 1D amplifier (Molecular Devices, Sunnyvale, CA) and a Digidata 1322 acquisition board (Molecular Devices). pClamp software, version 9 (Molecular Devices) was used for data acquisition. Electrodes had resistances of 4-6 MΩ. In all instances, cells were excluded from analysis if a leak current >200 pA was observed.

For recording, the culture medium was exchanged for a saline solution containing (in mM): 138 NaCl, 4 KCl, 2 $CaCl_2$, 1 $MgCl_2$, 10 glucose, 10 HEPES, and 0.025 D-2-Amino-5-phosphonovalerate (D-APV), pH 7.25. For Ca^{2+} current recordings, 3 mM Ba^{2+} was used as the charge carrier to increase the current size and to improve the passive properties of the cell. Also, 500 nM tetrodotoxin (TTX), 1 μM 2,3-dihydroxy-6-nitro-7-sulfonyl-benzo[f]quinoxaline (NBQX), and 25 μM bicuculline were included to block sodium currents and spontaneous synaptic currents. All Ba^{2+} currents were digitally subtracted using a trace recorded in the presence of 50 μM Cd^{2+}. The whole-cell pipette contained (in mM):

140 cesium methanesulfonate, 4 NaCl, 0.5 $CaCl_2$, 5 EGTA, 10 HEPES, pH 7.25. Cells were stimulated with 50 ms pulses to 0 mV from the holding potential of -70 mV. Capacitance was estimated as described previously (Xu et al. 2000; Moulder et al. 2002).

Treatment with drugs and assessment of caspase activity and cell death

Cultures were treated with proteasome inhibitors and other drugs in Minimal Essential Media (MEM; with Earle's salts, with 2 mM glutamine and 25 mM glucose) in a 5% CO_2 incubator maintained at 37°C. Following the treatment period (typically 48 hr), cell death was analyzed using propidium iodide (PI) fluorescence or by analyzing efflux of lactate dehydrogenase (LDH) into the bathing media as previously described (Trost and Lemasters 1994; Sattler et al. 1997; Snider et al. 2002).

Caspase activity was analyzed by measuring degradation of a fluorogenic caspase-3 substrate, acetyl-Asp-Glu-Val-Asp-7-amido-4-methylcoumarin (Ac-DEVD-AMC) using a commercially available kit (Sigma Chemical Co., Saint Louis, MO). Cleavage of the substrate results in the release of the aminomethylcoumarin (AMC) fluorescent moiety. The assays were performed in a microplate format as recommended by the manufacturer. Background activity (activity not inhibited by addition of 2 μM Acetyl-Asp-Glu-Val-Asp-al, a caspase inhibitor) was subtracted.

Replication and Statistics

Unless otherwise noted, all data reported here represent at least n= 12 sister cultures (each sister culture is a culture well) from at least three independent replications. Data were analyzed for significance ($P<0.05$) by ANOVA and Bonferroni post-hoc test for multiple comparisons.

Results

$[Ca^{2+}]_i$ is reduced during the early, reversible stages of proteasome inhibitor-induced neuronal death

We studied neuronal death occurring over 24-48 hr of moderate proteasome inhibition. We have previously shown that neuronal cultures treated with 3 μM MG-132 have about a 50% reduction in proteasome activity as compared to sham-washed cultures; 1 μM MG-132 reduces proteasome activity by 30-40% (Snider et al. 2002); this is similar to the level of proteasome impairment observed in brain regions affected by neurodegenerative disorders (Keller et al. 2000; McNaught and Jenner 2001; Keck et al. 2003). This process has many features of programmed cell death, including morphological changes such as cell body shrinkage and nuclear condensation and sensitivity to inhibition of protein and DNA synthesis and caspases (Qiu et al. 2000; Snider et al. 2002). As shown in Figure 1A (red lines), cultured neocortical neurons treated with MG- 132 (1 μM), a reversible proteasome inhibitor, began to die after about 24 hr treatment and were almost all killed by 44 hr treatment. Similar results were obtained with 3 μM MG-132 (data not shown). There was no significant death in sham-washed cultures over the 48 hr period. We next examined the time course of activation of caspase-3, a cysteine protease that plays a key role in many forms of programmed cell death (Jacobsen et al. 1996). Blue lines in Figure 1A show that, as expected, caspase-3 activity in MG-132 treated cultures increased after 12 hr treatment, before cell death was detectable, with a maximal increase at 24 hr, the last time point assessed.

We next measured free cytosolic Ca^{2+} ($[Ca^{2+}]_i$, black line in Figure 1A) during treatment with proteasome inhibitor. $[Ca^{2+}]_i$ remained stable in sham-washed cultures immediately after washing (also see Figure 1B) and throughout the 24 hr observation period (data not

shown) . The estimated $[Ca^{2+}]_i$ in sham-washed cultures averaged 119 ± 9.5 nM, similar to previous studies. $[Ca^{2+}]_i$ did not change immediately after application of MG-132 (Figure 1C), but was decreased after 4 hr (black lines in Figure 1A), to an estimated value of 101 ± 2.9 nM (85% of control, *P<0.05*). After 8 hr treatment with proteasome inhibitor, $[Ca^{2+}]_i$ was reduced to 49 ± 4 nM (41% of control, *P<0.001)*. This decrease in $[Ca^{2+}]_i$ was transient as $[Ca^{2+}]_i$ in MG-132-treated cultures increased to 146 ± 19 nM after 16 hr (not significantly different than sham-washed cultures). We did not measure $[Ca^{2+}]_i$ or caspase activation at time points > 24 hr as some of the cells began to lose membrane integrity and loading and retention of dye was compromised. This reduction in $[Ca^{2+}]_i$ thus began before activation of caspase-3 and before neuronal death was detectable by propidium iodide fluorescence.

Calcium influx via voltage gated Ca^{2+} channels can attenuate proteasome inhibitor-induced injury even if delayed up to 16 hr

We have previously reported that co-application of the calcium channel agonist (-) Bay K8644(BayK) throughout a 48 hr treatment attenuates proteasome inhibitor-induced neuronal death, while blockade of NMDA-subtype glutamate receptor mediated Ca^{2+} influx with NMDA receptor antagonists (MK-801, D-APV) increases this death (Snider et al. 2002). We now show that co-application of the glutamate receptor agonist kainate (KA) increased $[Ca^{2+}]_i$ in sham-washed cultures and reversed the MG-132 induced decrease in $[Ca^{2+}]_i$ (Figure 2). The increase in $[Ca^{2+}]_i$ observed with KA is similar to that we have reported for BayK, and both compounds reversed the reduction in $[Ca^{2+}]_i$ caused by proteasome inhibitors (compare Figure 2A here with Figure 7A in Snider et al., 2002). We reasoned that increasing $[Ca^{2+}]_i$ using BayK or KA would only attenuate neuronal death if the Ca^{2+}-raising agent was added during the critical time period when Ca^{2+} was reduced. We tested this hypothesis by delaying the timing of addition of KA or BayK. Cultures were treated with proteasome inhibitor for 48 hr as in Figure 1. (-) Bay K8644 (10 μM) or kainate (10 μM) were present throughout the treatment period in the (0 hr) condition, or added at the indicated time 4-20 hr after the start of the treatment period. Cell death was analyzed at the end of the 48 hr exposure. BayK attenuated proteasome inhibitor-induced neuronal death even when added 20 hr after the start of the 48 hr treatment period; later application (≥ 24 hr) did not reduce neuronal death. Addition of kainate (KA, 10 μM) also attenuated cell death when added up to 16 hr after the start of treatment (Figure 2B). We did not test addition at time points later than 24 hr since significant neuronal death was already detectable at that time (Figure 1). Treatment with BayK or kainate alone for 48 hr did not result in detectable neuronal death (data not shown).

MG-132 is relatively non-specific reversible proteasome inhibitor, so we analyzed $[Ca^{2+}]_i$ in neuronal cultures after 4 hr treatment with clastolactacystin β-lactone, a highly specific irreversible proteasome inhibitor (Dick et al. 1997; Fenteany and Schreiber 1998). We observed a reduction in $[Ca^{2+}]_i$ similar to that seen with MG-132. 340/380 nm ratio for sham-washed cultures was 0.972 ± 0.024, compared to 0.825 ± 0.035 for cultures treated with 3 μM clastolactacystin (differs significantly by ANOVA, $P<0.001$). Estimated $[Ca^{2+}]_i$ was 120 ± 6.4 nM in sham-washed cultures; this was reduced to 82.0 ± 10.1 nM in clastolactacystin-treated cultures (data not shown). Consistent with our previous observations (Snider et al. 2002), co-application of 10 μM BayK modestly reduced neuronal death caused by 48 hr treatment with 3 μM clastolactacystin. Kainate did not significantly reduce this death, but kainate did block the ability of NMDA receptor antagonists to potentiate clastolactacystin-induced neuronal death (Supplemental Figure 1). NMDA antagonists alone were not toxic under these conditions, although toxicity has been reported in a similar culture system (Hwang et al. 1999).

We have previously reported that reductions in $[Ca^{2+}]_i$, either by treatment with Ca^{2+}-free media or with the Ca^{2+}-chelator BAPTA, cause a caspase-dependent death in cultured

cortical neurons (Canzoniero et al. 2004). The period during which application of Ca^{2+}-raising agents is neuroprotective overlaps with that during which $[Ca^{2+}]_i$ is reduced (compare Figure 2B to Figure 1A) and parallels the timing of caspase activation, consistent with the idea that caspase activation represents the "commitment point" beyond which cell death is inevitable. We confirmed that co-application of BayK blocked caspase activation by measuring caspase activity 24 hr after the start of MG-132 treatment in the presence or absence of BayK. In this series of experiments, caspase activity was 4321 ± 486 pmol/μg/min after 24 hr treatment with 1 μM MG-132; this increase was nearly completely blocked by the co-application of 10 μM BayK (caspase activity after 24 hr in BayK+ MG cultures was 161 ± 16 pmol/μg/min, differs from MG-132 alone $P<0.001$; for comparison, caspase activity in sham-washed cultures after 24 hr was 72 ± 1 pmol/μg/min, data not shown).

Increasing calcium influx via the Na-Ca exchanger attenuates proteasome inhibitor-induced neuronal death

These findings suggest that the reduction in $[Ca^{2+}]_i$ may be an important, potentially reversible event that ultimately contributes to proteasome inhibitor-induced neuronal death. Both BayK and kainate elevate $[Ca^{2+}]_i$ by increasing Ca^{2+} entry through L-type voltage-gated Ca^{2+} channels. Another major route of Ca^{2+} flux in neuronal cells is the plasma membrane Na-Ca exchanger (NCX). The exchanger is bidirectional; it can reduce $[Ca^{2+}]_i$ in "forward mode" by transferring Ca^{2+} out of the cell in exchange for Na^+, or increase cytoplasmic Ca^{2+} in "reverse mode." The role of the exchanger in maintaining Ca^{2+} homeostasis under resting conditions remains unclear, but a control experiment demonstrated that cultures treated with the NCX inhibitor benzamil (10 μM for 4 hr) had an increase in $[Ca^{2+}]_i$, suggesting that the exchanger functions predominantly in "forward mode" (transferring Ca^{2+} out of the cell) under resting conditions (Figure 3, Sham condition at left). In cultures treated with the proteasome inhibitor MG-132, the addition of benzamil normalized $[Ca^{2+}]_i$ so that $[Ca^{2+}]_i$ after 4 hr treatment was not significantly different from that in sham-washed cultures. Such co-application of benzamil also reduced the neuronal death caused by 48 hr treatment with MG-132 (Figure 3, right panel) or with clastolactacystin (Supplemental Figure 1).

Proteasome inhibitors cause a reduction in Ca^{2+} influx via voltage-gated Ca^{2+} channels

The observation that proteasome inhibitors reduce $[Ca^{2+}]_i$ and that increasing Ca^{2+} influx can attenuate proteasome inhibitor induced death suggests that proteasome inhibitor treated cultures have reduced Ca^{2+} intake or increased Ca^{2+} efflux. We examined basal Ca^{2+} efflux and saw no significant differences in proteasome-inhibitor treated cells, although there was a trend toward reduced basal Ca^{2+} efflux in proteasome inhibitor-treated neurons (Supplemental Figure 2). We next investigated whether proteasome inhibitors altered Ca^{2+} influx via voltage-gated Ca^{2+} channels. As shown in Figure 4A, proteasome inhibitor-treated neurons had a reduction in amplitude of currents through voltage-gated Ca^{2+} channels. There was no effect seen when only L-type channels were examined, suggesting this effect is mediated by other types of voltage-gated Ca^{2+} channels (e.g., N, P,Q, R or T type channels). We also observed a smaller increase in $[Ca^{2+}]_i$ during depolarization in proteasome inhibitor-treated than in sham-washed neurons, a result consistent with reduced Ca^{2+} influx via voltage gated Ca^{2+} channels (Figure 4C).

ER Ca^{2+} is also reduced following treatment with proteasome inhibitor

The reduction in $[Ca^{2+}]_i$ caused by proteasome inhibitor may in part reflect a reduction in Ca^{2+} influx, but redistribution of Ca^{2+} from cytosol into other cellular compartments could also contribute. For example, a toxic redistribution of Ca^{2+} from cytosol to ER and ultimately to mitochondria has been reported in cultured neurons treated with ceramide (Darios et al. 2003; Darios et al. 2005). We directly measured ER Ca^{2+} ($[Ca^{2+}]_{ER}$) using the

low affinity dye mag-fura-2. We confirmed that mag-fura-2 ratios reflected ER Ca^{2+} levels by showing that thapsigargin (2.5 μM for 30 min) reduced the putative $[Ca^{2+}]_{ER}$ signal by about 50% (see Supplemental Figure 3A), similar to previous reports using this method in cultured neurons (Darios et al. 2005). In addition, permeabilization of the plasma membrane with digitonin (10 μM) reduced fura-2 fluorescence to background levels, while the mag-fura-2 signal was only slightly decreased, consistent with localization of most of the mag-fura-2 signal within organelles such as the ER (Supplemental Figure 3B). As shown in Figure 5A, $[Ca^{2+}]_{ER}$ in cultures treated with proteasome inhibitor for 4 hr was reduced and reached a nadir at 8 hr, then returned to baseline levels by 16 hr, a pattern identical to that observed for $[Ca^{2+}]_i$.

We also examined ER Ca^{2+} levels indirectly by analyzing changes in $[Ca^{2+}]_i$ after blockade of ER Ca^{2+} uptake with thapsigargin (5 μM). Thapsigargin was added to cultures in nominally Ca^{2+}-free media to eliminate increases in Ca^{2+} from extracellular sources. Using this method, we observed a robust thapsigargin-stimulated increase in $[Ca^{2+}]_i$ in sham-washed cultures, but not in cultures treated with proteasome inhibitor for 4 or 16 hr (Figure 5B). After $[Ca^{2+}]_i$ reached steady state, Ca^{2+} was added to the extracellular media and $[Ca^{2+}]_i$ increased, consistent with influx via the store-activated channels. The increase in $[Ca^{2+}]_i$ after addition of extracellular Ca^{2+} was blunted in cultures treated with proteasome inhibitor for 4 hr, but had recovered by 16 hr. Proteasome-inhibitor treated cultures thus have reduced levels of Ca^{2+} in the ER and, at least early in the injury, likely have reduced capacitative Ca^{2+} entry to refill these depleted stores.

Proteasome inhibitor-treated neurons have modestly increased levels of mitochondrial Ca^{2+}

We next looked at the role of mitochondrial Ca^{2+} because mitochondria provide an important high capacity, low affinity cellular Ca^{2+} store. We measured mitochondrial Ca^{2+} ($[Ca^{2+}]_{mito}$) indirectly by monitoring fura-2 fluorescence before and after the application of the protonophore carbonyl cyanide 4-(trifluoromethoxy)phenylhydrazone (FCCP, 10 μM), a maneuver that dissipates the mitochondrial proton gradient and releases mitochondrial Ca^{2+} (Thayer and Miller 1990; Brocard et al. 2001). Neuronal cultures were treated with MG-132 and then changed to Ca^{2+}-free buffer prior to imaging. Sham-washed cultures had little change in $[Ca^{2+}]_i$ after exposure to FCCP (gray line in Figure 6A; basal $[Ca^{2+}]_i$ in control cultures was 100 ± 6 nM, increasing to a maximum of 124 ± 8 nM after FCCP), consistent with previous reports using similar methods in rat forebrain cultures (Brocard et al. 2001). In contrast, cultures treated with proteasome inhibitor (MG-132, 2 μM for 4 hr) had a lower resting $[Ca^{2+}]_i$ than control cultures (similar to the decrease shown in Figure 1A and our previous studies) but elevated $[Ca^{2+}]_i$ after treatment with FCCP, consistent with increased Ca^{2+} release from mitochondrial stores (maximum $[Ca^{2+}]_i$ estimated at 230 nM, black line Figure 6A). For comparison, we analyzed $[Ca^{2+}]_{mito}$ in neurons treated with 300 μM NMDA for 10 min; this treatment causes a rapidly evolving neuronal death triggered in part by mitochondrial Ca^{2+} overload (Nicholls 2004). As expected, basal $[Ca^{2+}]_i$ was increased in NMDA-treated cells (to an estimated level of about 1.05 μM) and $[Ca^{2+}]_i$ increased massively after application of FCCP (Figure 6B). The NMDA-induced increase in $[Ca^{2+}]_{mito}$ was much greater than that observed in cultures treated with MG-132 (same data for MG-132 shown in 6A and 6B, but scaling is different). These values likely underestimate the increase in NMDA-treated cells because fura-2, a relatively high affinity dye, may have reached saturation. Thus, although there is an increase in mitochondrial Ca^{2+} in proteasome inhibitor-treated cultures, this increase is of a much lower magnitude than that seen in cultures treated with NMDA, a situation in which mitochondrial Ca^{2+} overload likely plays an important role in cell death.

Role of mitochondrial Ca^{2+} in neuronal death caused by proteasome inhibitor

As noted above, the increases in $[Ca^{2+}]_{mito}$ observed in proteasome inhibitor-treated neurons were small and might not be physiologically significant. We addressed this issue by testing the effect of ruthenium red (RuR, 10 μM) on mitochondrial Ca^{2+} levels and neuronal death in proteasome inhibitor-treated cultures. RuR is a widely used, although potentially nonspecific and poorly cell permeable, antagonist of mitochondrial Ca^{2+} uptake via the uniporter (Lehninger et al. 1967). RuR has been reported to block the uniporter in cultured neurons (Wang and Thayer 2002). Cultured neurons were sham-washed or treated with RuR for 40 min; baseline cytoplasmic Ca^{2+} was measured with fura-2 and then mitochondrial Ca^{2+} was released with FCCP and cytoplasmic Ca^{2+} was measured again. As shown in Figure 6C, 40 min treatment with RuR (10 μM) increased basal $[Ca^{2+}]_i$ levels and abolished the ability of FCCP to further increase $[Ca^{2+}]_i$ under all conditions tested, consistent with blockade of mitochondrial Ca^{2+} uptake. The increase in $[Ca^{2+}]_i$ (in the absence of FCCP) in RuR-treated cultures likely reflects inhibition of basal mitochondrial Ca^{2+} uptake.

We next tested the effects of RuR treatment (pretreatment and co-application) on neuronal vulnerability to proteasome inhibitor and NMDA-induced neuronal death. Blockade of mitochondrial Ca^{2+} uptake would be expected to block mitochondrial Ca^{2+} overload. Co-application of RuR attenuated NMDA-induced neuronal death, but did not attenuate MG-132- or clastolactacystin-induced death (Figure 6D). Co-application of RuR also failed to attenuate less severe insults, such as 3 μM clastolactacystin treatment for 24 hr (43.9 ± 6.2% neuronal death alone; 41.7 ± 5.9% neuronal death with co-application of 10 μM RuR). RuR does not inhibit NMDA receptors at the concentrations used here, as evidenced by lack of effect on $[Ca^{2+}]_i$ when applied concurrently with NMDA (data not shown).

Mitochondria take up Ca^{2+} via the uniporter and then release it under physiological conditions via the mitochondrial Na-Ca exchanger. We tested the effect of inhibiting mitochondrial Ca^{2+} efflux on $[Ca^{2+}]_i$ and neuronal vulnerability to proteasome inhibitor-induced injury using CGP-37157, a highly specific inhibitor of the mitochondrial Na-Ca exchanger (Cox et al. 1993; White and Reynolds 1997). Treatment with 10 μM CGP-37157 did not significantly reduce $[Ca^{2+}]_i$, nor did treatment with a sublethal concentration of MG-132 (0.3 μM) (Figure 7A). Co-application of CGP-37157 and 0.3 μM MG-132 caused a significant reduction in $[Ca^{2+}]_i$ similar to that seen following treatment with higher, toxic concentrations of MG-132 (compare Figure 7A to Figures 1 and 2) and also potentiated MG-132 and clasto-lactacystin-induced neuronal death (Figure 7B-C). In contrast, co-application of CGP-37157 did not alter vulnerability to NMDA-induced death (7B, light gray line). Application of CGP-37157 alone caused no injury at concentrations up to 25 μM (data not shown).

Although astrocytes are less vulnerable to proteasome inhibitor-induced death than neurons (Snider et al. 2002), some of the effects of Ca^{2+} altering strategies on neuronal vulnerability could be mediated indirectly by astrocytes in these mixed neuronal-astrocyte cultures. “Pure” neuronal cultures containing >95% neurons were more sensitive to proteasome inhibitors (MG-132 LD_{50} ~ 0.1 μM) than cultures containing both neurons and astrocytes MG-132 LD_{50} 1-3 μM) but, similar to mixed astrocyte-neuronal cultures, proteasome inhibitor-induced death in pure neuronal cultures was attenuated by co-application of (-) Bay K8644 (10 μM) or benzamil (10 μM) and exacerbated by co-application of CGP-37157 (10 μM). Co-application of kainate did not reduce neuronal death, but this could in part be due to the increased vulnerability of these cultures to excitotoxic neuronal injury.

Discussion

We report here that cultured neurons treated with proteasome inhibitors had reduced cytosolic and ER Ca^{2+} levels 4-8 hr after the start of the injury, before or concurrent with activation of caspase-3 and before cell death was detectable by propidium iodide staining. We show a reduction in voltage-gated Ca^{2+} channel current density and in the depolarization-stimulated increase in $[Ca^{2+}]_i$ in proteasome inhibitor-treated neurons, and show that maneuvers that increase Ca^{2+} influx via the voltage-gated Ca^{2+} channel or the Na-Ca^{2+} exchanger blocked the decrease in Ca^{2+} levels and reduced cell death. The "therapeutic window" for application of compounds that increased Ca^{2+} entry via the voltage-gated Ca^{2+} channel corresponds roughly to the time period of reduced cellular Ca^{2+} and ended as caspases were activated. These findings suggested that proteasome inhibitor-induced neuronal death is mediated by a reduction in Ca^{2+} influx that may be in part due to dysfunction of voltage-gated Ca^{2+} channels and an overall cellular Ca^{2+} deficiency. Interestingly, proteasome inhibitor treatment did not alter current density of L-type voltage-gated Ca^{2+} channels, so the inhibitory effects of proteasome inhibition may be on N, P, Q, R or T type channels. The protective effects of (-) Bay K8644, an L-type channel agonist, were consistent with the idea that L-type channels remain functional in proteasome-inhibitor treated cells.

Both a reversible (MG-132) and a more specific irreversible (clastolactacystin β-lactone) proteasome inhibitor reduced neuronal $[Ca^{2+}]_i$. Neuronal death induced by these inhibitors was similarly attenuated by co-application of BayK8644 and benzamil and exacerbated by NMDA antagonists. There was a difference in the effects of co-application of kainate; kainate modestly attenuated neuronal death caused by MG-132 (Figure 2B) but the injury-reducing effects of kainate against clastolactacystin-induced death did not achieve statistical significance (compare Figure 2B and Supplemental Figure 1).

To our knowledge, this is the first study to assess $[Ca^{2+}]_{ER}$ and $[Ca^{2+}]_{mito}$ in cells undergoing insults associated with a reduction in $[Ca^{2+}]_i$. We initially hypothesized that the reduction in cytosolic $[Ca^{2+}]_i$ would be accompanied by increased sequestration of Ca^{2+} in ER and mitochondria; this was clearly not the case for ER Ca^{2+} as it was reduced to a similar extent as $[Ca^{2+}]_i$. Store-operated Ca^{2+} uptake was impaired after 4 hr treatment with proteasome inhibitor and was restored after 16 hr, raising the possibility that a defect in coupling of ER and cytosolic Ca^{2+} levels to capacitative Ca^{2+} entry underlies the derangement in Ca^{2+} homeostasis in proteasome inhibitor-treated neurons.

An increase, rather than a decrease, in $[Ca^{2+}]_i$ has been reported during the first hr of treatment with proteasome inhibitors in undifferentiated PC12 cells or myeloma cells (Landowski et al. 2005; Lee et al. 2005). We did not observe any increase in $[Ca^{2+}]_i$ in proteasome inhibitor treated neurons (Figure 1B-C). Interestingly, the acute increase in $[Ca^{2+}]_i$ observed in myeloma cells was followed by an apparent reduction in $[Ca^{2+}]_i$ over the next 30 min (see Landowski et al. 2005). It is thus possible that proteasome inhibitor-mediated toxicity in other cell types may also be mediated by a reduction in $[Ca^{2+}]_i$.

We considered the possibility that mitochondrial Ca^{2+} overload might play a role in proteasome inhibitor-induced death, perhaps through transfer of Ca^{2+} from cytosol and ER to mitochondria as suggested by Darios et al. for ceramide-induced neuronal death (2003; 2005). Although we observed a modest increase in $[Ca^{2+}]_{mito}$ in neurons undergoing proteasome inhibitor-induced neuronal death, the magnitude of increase in $[Ca^{2+}]_{mito}$ was much lower than that seen following a toxic NMDA treatment and blockade of mitochondrial Ca^{2+} uptake via the uniporter with ruthenium red did not reduce proteasome inhibitor-induced death, in contrast to the effects of ruthenium red in NMDA-treated

neurons (Figures 6B and 6D). Conversely, blockade of mitochondrial Ca^{2+} efflux with CGP-37157 increased proteasome inhibitor-induced neuronal death but did not alter vulnerability to NMDA (Figure 7B), suggesting that mitochondrial Ca^{2+} uptake might contribute to proteasome inhibitor induced death by sequestering Ca^{2+} from other compartments rather than by a toxic effect on mitochondria.

The injury-reducing effects of increased Ca^{2+} entry were not restricted to entry via voltage-gated Ca^{2+} channels, as MG-132 and clastolactacystin-induced neuronal death was also reduced by co-application of benzamil, a relatively nonspecific blocker of the plasma-membrane Na-Ca exchanger. Although nonspecific effects of this compound cannot be ruled out, these studies are consistent with the idea that reductions in $[Ca^{2+}]_i$ play a role in cell death.

There are some potential confounds with the measures of Ca^{2+} used here, particularly the measures of ER and mitochondrial Ca^{2+}. We imaged $[Ca^{2+}]$ in cell bodies; alterations in cytosolic, ER and mitochondrial Ca^{2+} in neuronal processes are likely to play an important role in neuronal survival and were not assessed in these studies. Mag-fura-2 also binds Mg^{2+} (K_D ~ 1.5 mM for Mg^{2+} as compared to ~ 50-190 μM for Ca^{2+}) so some of the signal detected could possibly reflect Mg^{2+} rather than Ca^{2+} (Raju et al. 1989; Hyrc et al. 2000) . However, studies in astrocytes and myocytes have shown that this dye is relatively selective for Ca^{2+} at concentrations > 50 μM (Golovina and Blaustein 1997). There can be averaging of signal between compartments with higher (e.g., ER) and those with lower Ca^{2+} (e.g., cytosol) so this technique may underestimate $[Ca^{2+}]_{ER}$ (Hyrc et al. 2007), but such averaging is unlikely to account for the observed decrease in $[Ca^{2+}]_{ER}$ in proteasome inhibitor-treated cultures.

The use of FCCP-mediated depolarization to assess mitochondrial Ca^{2+} also has potential drawbacks; for example, FCCP could cause acidification (Wang et al. 1995; White and Reynolds 1997) or plasma membrane depolarization (Buckler and Vaughan-Jones 1998). Despite the potential confounds, the increase in $[Ca^{2+}]_i$ seen acutely after application of FCCP has been widely used as an indirect measurement of $[Ca^{2+}]_{mito}$ in cultured cortical neurons. The concentration of FCCP used here (10 μM) is relatively high, but within the range of concentrations (0.75 – 10 μM) used in other studies of cultured neurons (Duchen et al. 1990; Thayer and Miller 1990; Kiedrowski and Costa 1995; Reynolds and Hastings 1995; Brocard et al. 2001). We observed similar results using 1 μM FCCP. We used fura-2 here rather than a lower affinity dye in order to measure the relatively modest increases in $[Ca^{2+}]_{mito}$ seen following proteasome inhibitor treatment. The disadvantage of this approach is that we likely underestimated the NMDA-induced increase in $[Ca^{2+}]_{mito}$.

Taken together, these observations support a model in which neurons undergoing proteasome inhibitor-induced neuronal death have an overall Ca^{2+} deficiency so that increasing Ca^{2+} entry from extracellular sources provides neuroprotection and blocking Ca^{2+} entry with glutamate antagonists or blocking mitochondrial Ca^{2+} release with CGP-37157 exacerbates injury. The contribution of Ca^{2+} deficiency to neuronal death occurs during the early steps of the cell death cascade before the activation of caspases and commitment to die. We hypothesize that proteasome inhibition impairs uptake via voltage-gated Ca^{2+} channels, perhaps via multiple N, P,Q, R or T type channels, but not through L-type channels. Proteasome inhibition may perturb normal homeostatic mechanisms that regulate capacitative Ca^{2+} entry. These findings raise the possibility that Ca^{2+} deficiency, rather than Ca^{2+} overload, may contribute to neuronal death in disorders where programmed cell death pathways are activated or proteasomal protein degradation pathways are impaired. Such a situation may occur in peripheral nerve or CNS in patients treated with proteasome inhibitors (e.g., for multiple myeloma), or perhaps in neurodegenerative disorders, although

the role of proteasome impairment in these disorders has not yet been established and these disorders evolve over years rather than hours. Further studies of proteasome inhibition and intracellular Ca^{2+} deficiency in neurological disorders are important as some currently contemplated therapeutic strategies, such as glutamate receptor antagonists, could increase neuronal injury during the early Ca^{2+}-deficient period, while treatments that increase Ca^{2+} influx could prove unexpectedly effective in delaying neuronal death.

Supplementary Material

Refer to Web version on PubMed Central for supplementary material.

Acknowledgments

This work was supported by the NIH/NINDS R01 NS44923 (BJS), NIH Neuroscience Blueprint Core Grant P30 NS057105 to Washington University and by the Charles and Joanne Knight Alzheimer Research Initiative of Washington University's Alzheimer's Disease Research Center. We thank Dr. Eugene M. Johnson, Jr., for his helpful comments on the manuscript.

Abbreviations used

(AMC)	aminomethylcoumarin
(BayK)	(-)Bay-K8644
(Ca^{2+})	calcium
(FCCP)	carbonyl cyanide 4-(trifluoromethoxy)phenylhydrazone
(ER)	endoplasmic reticulum
($[Ca^{2+}]_i$)	free cytosolic Ca^{2+} concentration
($[Ca^{2+}]_{ER}$)	free ER Ca^{2+} concentration
($[Ca^{2+}]_{mito}$)	free mitochondrial Ca^{2+} concentration
(UPS)	ubiquitin proteasome system

REFERENCES

Arundine M, Tymianski M. Molecular mechanisms of glutamate-dependent neurodegeneration in ischemia and traumatic brain injury. Cell Mol Life Sci. 2004; 61:657–668. [PubMed: 15052409]

Berliocchi L, Bano D, Nicotera P. Ca^{2+} signals and death programmes in neurons. Philos.Trans. R. Soc. Lond. B Biol. Sci. 2005; 360:2255–2258. [PubMed: 16321795]

Brocard JB, Tassetto M, Reynolds IJ. Quantitative evaluation of mitochondrial calcium content in rat cortical neurones following a glutamate stimulus. J. Physiol. 2001; 531:793–805. [PubMed: 11251059]

Buckler KJ, Vaughan-Jones RD. Effects of mitochondrial uncouplers on intracellular calcium, pH and membrane potential in rat carotid body type I cells. J. Physiol. 1998; 513(Pt 3):819–833. [PubMed: 9824720]

Canzoniero LM, Babcock DJ, Gottron FJ, et al. Raising intracellular calcium attenuates neuronal apoptosis triggered by staurosporine or oxygen-glucose deprivation in the presence of glutamate receptor blockade. Neurobiol. Dis. 2004; 15:520–528. [PubMed: 15056459]

Cox DA, Conforti L, Sperelakis N, et al. Selectivity of inhibition of $Na^{(+)}$-Ca^{2+} exchange of heart mitochondria by benzothiazepine CGP-37157. J. Cardiovasc. Pharmacol. 1993; 21:595–599. [PubMed: 7681905]

Darios F, Lambeng N, Troadec JD, et al. Ceramide increases mitochondrial free calcium levels via caspase 8 and Bid: role in initiation of cell death. J. Neurochem. 2003; 84:643–654. [PubMed: 12562509]

Darios F, Muriel M-P, Khondiker ME, et al. Neurotoxic Calcium Transfer from Endoplasmic Reticulum to Mitochondria Is Regulated by Cyclin-Dependent Kinase 5-Dependent Phosphorylation of Tau. J. Neurosci. 2005; 25:4159–4168. [PubMed: 15843619]

Dick LR, Cruikshank AA, Destree AT, et al. Mechanistic studies on the inactivation of the proteasome by lactacystin in cultured cells. J. Biol. Chem. 1997; 272:182–188. [PubMed: 8995245]

Duchen MR, Valdeolmillos M, O'Neill SC, et al. Effects of metabolic blockade on the regulation of intracellular calcium in dissociated mouse sensory neurones. J. Physiol. 1990; 424:411–426. [PubMed: 2391656]

Fenteany G, Schreiber SL. Lactacystin, proteasome function, and cell fate. J. Biol. Chem. 1998; 273:8545–8548. [PubMed: 9535824]

Golovina VA, Blaustein MP. Spatially and functionally distinct Ca^{2+} stores in sarcoplasmic and endoplasmic reticulum. Science. 1997; 275:1643–1648. [PubMed: 9054358]

Grynkiewicz G, Poenie M, Tsien RY. A new generation of Ca^{2+} indicators with greatly improved fluorescence properties. J. Biol. Chem. 1985; 260:3440–3450. [PubMed: 3838314]

Hwang JY, Kim YH, Ahn YH, et al. N-Methyl-D-aspartate receptor blockade induces neuronal apoptosis in cortical culture. Exp. Neurol. 1999; 159:124–130. [PubMed: 10486181]

Hyrc KL, Bownik JM, Goldberg MP. Ionic selectivity of low-affinity ratiometric calcium indicators: mag-Fura-2, Fura-2FF and BTC. Cell Calcium. 2000; 27:75–86. [PubMed: 10756974]

Hyrc KL, Rzeszotnik Z, Kennedy BR, et al. Determining calcium concentration in heterogeneous model systems using multiple indicators. Cell Calcium. 2007

Jacobsen MD, Weil M, Raff MC. Role of Ced-3/ICE-family proteases in staurosporine-induced programmed cell death. J. Cell Biol. 1996; 133:1041–1051. [PubMed: 8655577]

Johnson EM Jr. Koike T, Franklin J. A "calcium set-point hypothesis" of neuronal dependence on neurotrophic factor. Exp. Neurol. 1992; 115:163–166. [PubMed: 1728563]

Keck S, Nitsch R, Grune T, et al. Proteasome inhibition by paired helical filament-tau in brains of patients with Alzheimer's disease. J. Neurochem. 2003; 85:115–122. [PubMed: 12641733]

Keller JN, Hanni KB, Markesbery WR. Impaired proteasome function in Alzheimer's disease. J. Neurochem. 2000; 75:436–439. [PubMed: 10854289]

Kiedrowski L, Costa E. Glutamate-induced destabilization of intracellular calcium concentration homeostasis in cultured cerebellar granule cells: role of mitochondria in calcium buffering. Mol Pharmacol. 1995; 47:140–147. [PubMed: 7838122]

Landowski TH, Megli CJ, Nullmeyer KD, et al. Mitochondrial-mediated disregulation of Ca2+ is a critical determinant of Velcade (PS-341/bortezomib) cytotoxicity in myeloma cell lines. Cancer Res. 2005; 65:3828–3836. [PubMed: 15867381]

Lee CS, Han ES, Han YS, et al. Differential effect of calmodulin antagonists on MG132-induced mitochondrial dysfunction and cell death in PC12 cells. Brain Res. Bull. 2005; 67:225–234. [PubMed: 16144659]

Lee CS, Tee LY, Warmke T, et al. A proteasomal stress response: pretreatment with proteasome inhibitors increases proteasome activity and reduces neuronal vulnerability to oxidative injury. J. Neurochem. 2004; 91:996–1006. [PubMed: 15525353]

Lehninger AL, Carafoli E, Rossi CS. Energy-linked ion movements in mitochondrial systems. Adv. Enzymol. Relat. Areas Mol. Biol. 1967; 29:259–320. [PubMed: 4881885]

McNaught KS, Jenner P. Proteasomal function is impaired in substantia nigra in Parkinson's disease. Neurosci. Lett. 2001; 297:191–194. [PubMed: 11137760]

Moulder KL, Fu T, Melbostad H, et al. Ethanol-induced death of postnatal hippocampal neurons. Neurobiol. Dis. 2002; 10:396–409. [PubMed: 12270700]

Nawrocki ST, Carew JS, Pino MS, et al. Bortezomib sensitizes pancreatic cancer cells to endoplasmic reticulum stress-mediated apoptosis. Cancer Res. 2005a; 65:11658–11666. [PubMed: 16357177]

Nawrocki ST, Carew JS, Dunner K Jr. et al. Bortezomib inhibits PKR-like endoplasmic reticulum (ER) kinase and induces apoptosis via ER stress in human pancreatic cancer cells. Cancer Res. 2005b; 65:11510–11519. [PubMed: 16357160]

Nicholls DG. Mitochondrial dysfunction and glutamate excitotoxicity studied in primary neuronal cultures. Curr. Mol. Med. 2004; 4:149–177. [PubMed: 15032711]

Qiu JH, Asai A, Chi S, et al. Proteasome inhibitors induce cytochrome c-caspase-3-like protease-mediated apoptosis in cultured cortical neurons. J. Neurosci. 2000; 20:259–265. [PubMed: 10627603]

Raju B, Murphy E, Levy LA, et al. A fluorescent indicator for measuring cytosolic free magnesium. Am. J. Physiol. 1989; 256:C540–548. [PubMed: 2923192]

Ravin R, Spira ME, Parnas H, et al. Simultaneous measurement of intracellular Ca^{2+} and asynchronous transmitter release from the same crayfish bouton. J. Physiol. 1997; 501(Pt 2):251–262. [PubMed: 9192298]

Reynolds IJ, Hastings TG. Glutamate induces the production of reactive oxygen species in cultured forebrain neurons following NMDA receptor activation. J. Neurosci. 1995; 15:3318–3327. [PubMed: 7751912]

Rose, K.; Choi, DW.; Goldberg, MP. Cytotoxicity in murine neocortical cell culture. In: Tyson, C.; Frazier, J., editors. In Vitro Biological Methods. Vol. Vol. 1A. Academic Press; San Diego, CA: 1993. p. 46-60.

Sattler R, Charlton MP, Hafner M, et al. Determination of the time course and extent of neurotoxicity at defined temperatures in cultured neurons using a modified multiwell plate fluorescence scanner. J. Cereb. Blood Flow Metab. 1997; 17:455–463. [PubMed: 9143228]

Snider BJ, Tee LY, Canzoniero LM, et al. NMDA antagonists exacerbate neuronal death caused by proteasome inhibition in cultured cortical and striatal neurons. Eur. J. Neurosci. 2002; 15:419–428. [PubMed: 11876769]

Solovyova N, Veselovsky N, Toescu EC, et al. $Ca^{(2+)}$ dynamics in the lumen of the endoplasmic reticulum in sensory neurons: direct visualization of $Ca^{(2+)}$-induced $Ca^{(2+)}$ release triggered by physiological $Ca^{(2+)}$ entry. EMBO J. 2002; 21:622–630. [PubMed: 11847110]

Thayer SA, Miller RJ. Regulation of the intracellular free calcium concentration in single rat dorsal root ganglion neurones in vitro. J. Physiol. 1990; 425:85–115. [PubMed: 2213592]

Trost LC, Lemasters JJ. A cytotoxicity assay for tumor necrosis factor employing a multiwell fluorescence scanner. Anal. Biochem. 1994; 220:149–153. [PubMed: 7978238]

Wang GJ, Thayer SA. NMDA-induced calcium loads recycle across the mitochondrial inner membrane of hippocampal neurons in culture. J. Neurophysiol. 2002; 87:740–749. [PubMed: 11826043]

Wang GJ, Richardson SR, Thayer SA. Intracellular acidification is not a prerequisite for glutamate-triggered death of cultured hippocampal neurons. Neurosci. Lett. 1995; 186:139–144. [PubMed: 7777183]

White RJ, Reynolds IJ. Mitochondria accumulate Ca^{2+} following intense glutamate stimulation of cultured rat forebrain neurones. J. Physiol. 1997; 498:31–47. [PubMed: 9023766]

Wu, S.; Hyrc, K.; Lin, Y., et al. Proteasome inhibitor-induced neuronal death is associated with low intracellular calcium: role of endoplasmic reticulum and mitochondrial calcium. Neuroscience Meeting Planner; Atlanta, GA. Society for Neuroscience, 2006. Online; 2006. Program No. 824.826

Xu W, Cormier R, Fu T, et al. Slow death of postnatal hippocampal neurons by GABA(A) receptor overactivation. J. Neurosci. 2000; 20:3147–3156. [PubMed: 10777778]

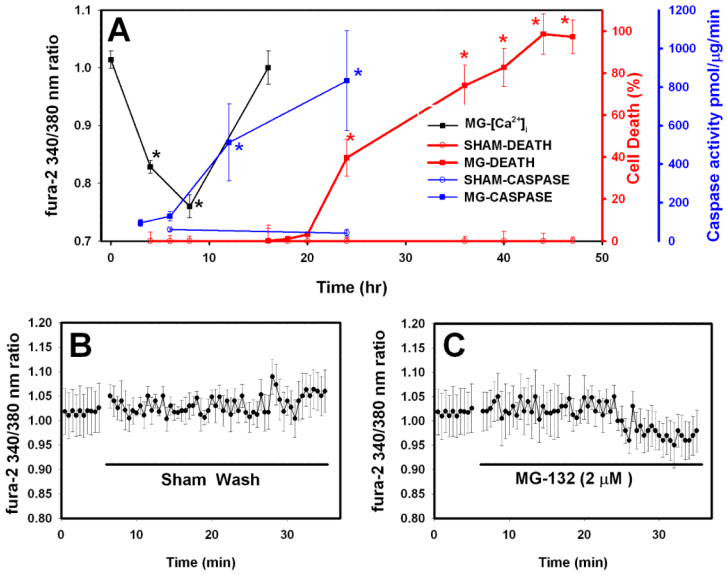

Figure 1. Time course of neuronal death, caspase activity and $[Ca^{2+}]_i$ following treatment with proteasome inhibitor (MG-132)

A. Cell death (red lines and symbols; Y-axis shown at right): Cultures were treated with proteasome inhibitors for 48 hr or sham-washed. Values shown are mean ± SEM cell death as assayed by propidium iodide fluorescence at the indicated time points. Values in sham-washed cultures were subtracted so death in sham-washed cultures =0%; there was no significant change in absolute fluorescence values for sham-washed cultures at any time point throughout the 48 hr treatment period. For all 3 measures shown in Panel A, * indicates death in MG-132-treated cultures differs significantly from that in sham-washed cultures; significance ($P<0.05$) was analyzed by ANOVA and Bonferroni post-hoc test. Caspase-3 activity (Blue line and symbols; Y-axis at far right): Cultures were treated as in the cell death assay. At the indicated time intervals after the start of the MG-132 treatment or sham wash, extracts were prepared and degradation of Ac-DEVD-AMC was determined. Values shown are mean ± SEM activity in pmol AMC cleaved/μg protein/min. Sham wash values did not differ significantly between any time points. Calcium imaging (Black line and symbols; Y-axis at left): cultures were sham-washed or treated with MG-132 and then returned to the incubator. At the indicated time after the start of drug treatment, cultures were loaded with fura-2 and images were collected. Values shown are mean ± SEM 340/380 ratios for n= 87-200 cells for each data point. Values shown are average of three consecutive measurements taken for each cell. MG-132 was included in the loading and washing buffers for treated cultures. B. Acute changes in $[Ca^{2+}]_i$. Cultures were loaded with fura-2 as in A. The solid line indicates when the cultures were sham washed. $[Ca^{2+}]_i$ was measured every 30 seconds for an additional 30 min after the sham wash. Values shown are mean ± SEM 340/380 ratio for 15 neurons in two separate experiments. C. Similar to B, but MG-132 (2 μM) was added at the indicated time. Values shown are mean ± SEM 340/380 ratio for 17 neurons in two separate experiments.

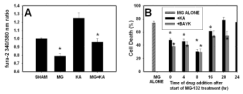

Figure 2. Activating Ca^{2+} influx via voltage gated Ca^{2+} channels prevents proteasome inhibitor-induced $[Ca^{2+}]_i$ depletion and attenuates neuronal death

A. Murine neocortical cultures were sham-washed (vehicle only) or treated with MG-132 (2 μM) in the presence or absence of kainate (10 μM) or with kainate alone. $[Ca^{2+}]_i$ was imaged after 4 hr. Values shown are mean ± SEM 340/380 ratios for n= 40 cells for each data point. * indicates significant difference ($P<0.05$) from SHAM condition. B. Murine neocortical cultures were treated with MG-132 (1 μM) for 48 hr. (-) Bay K8644 (BayK, 10 μM) or kainate (KA, 10 μM) was added at the beginning of the treatment period at the indicated time after the start of the treatment period. Compounds added at time "0" were co-applied with the MG-132 and were present throughout the treatment period. Values shown are mean ± SEM cell death analyzed at the end of the 48 hr treatment period. * indicates values for KA or BayK treated cultures differed significantly ($P<0.05$) from those of sister cultures treated with MG-132 alone.

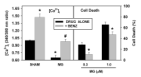

Figure 3. Blockade of the Na-Ca exchanger (NCX) increases $[Ca^{2+}]_i$ and reduces vulnerability to MG-132-induced neuronal death

Left panel: $[Ca^{2+}]_i$ measurements. Murine neocortical cultures were sham-washed (SHAM) or treated with benzamil (BENZ, 10 μM) for 4 hr in the absence (left two SHAM bars) or presence of MG-132 (MG, 1 μM) and then $[Ca^{2+}]_i$ was measured as in Figure 1A. * indicates values were significantly different ($P<0.05$ by ANOVA with Bonferroni post hoc) from those in sham-washed condition without benzamil (left most bar). # indicates that cultures with BENZ+MG-132 differed from those treated with MG-132 alone. Values for MG-132 cultures treated with BENZ did not differ significantly from those in sham-washed condition without BENZ. Right panel: Cultures were treated with MG-132 (MG, 0.3 or 1.0 μM) for 48 hr in the presence or absence of benzamil (BENZ, 10 μM). Values shown are mean ± SEM cell death as assayed by propidium iodide fluorescence at the end of the 48 hr treatment period. * indicates values in +BENZ condition differ significantly from treated with MG alone.

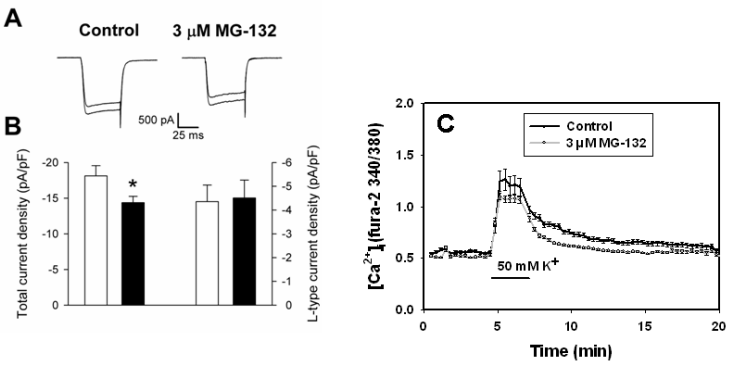

Figure 4. Effect of proteasome inhibitor treatment on voltage-gated Ca^{2+} channel currents and Ca^{2+} influx

A. Representative Ca^{2+} currents elicited by voltage steps from -70 to 0 mV in a neuron treated with control medium and a neuron treated with 3 μM MG-132 for 4 hr. Currents were recorded in each neuron in the absence (larger trace) and presence (smaller trace) of 5 μM nifedipine. The capacitance of the control neuron was 24.7 pF and that of the MG-132-treated neuron was 25.6 pF. B. Summary of the total Ca^{2+} current density (two left-most bars) and the Ca^{2+} current density carried by L-type channels (two right-most bars) in control (open bars) and MG-132-treated (filled bars) neurons. n = 11-12; **P* < 0.04. No statistically significant difference was observed in the L-type current density. C. Cultured neurons were sham-washed (Control) or treated with 3 μM MG-132 for 4 hr. Cultures were loaded with fura-2 and $[Ca^{2+}]_i$ was imaged as in Figure 1. After 5 min, cultures were changed into media supplemented with 50 mM K^+ for 2 min, then returned to control medium. Values shown are mean ± SEM 340/380 ratio for n= 96-100 cells per condition.

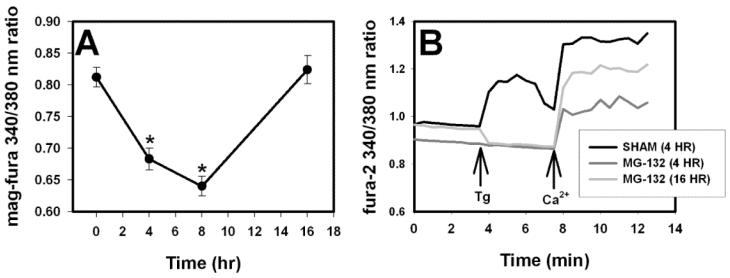

Figure 5. Effect of proteasome inhibitors on endoplasmic reticulum (ER) Ca^{2+} ($[Ca^{2+}]_{ER}$)

A. Measurement of $[Ca^{2+}]_{ER}$ with mag-fura-2. Cultures were treated with MG-132 (2 μM) and then loaded with mag-fura-2 (see *Methods*) and $[Ca^{2+}]_{ER}$ was analyzed at the indicated time points after the start of the treatment period; images and data analysis were similar to that for fura-2 in Figures 1 and 3. n= 87-143 cells per time point. * indicates significant difference ($P<0.05$ by ANOVA) from sham-washed (time = 0) condition. B. Indirect measurement of $[Ca^{2+}]_{ER}$ with fura-2 and thapsigargin. Cultures were treated with MG-132 (2 μM) for 4 hr or 16 hr (darker and lighter gray lines respectively) or sham-washed for 4 hr (black line). Cultures were loaded with fura-2; before imaging, the media was changed to calcium free buffer. Baseline $[Ca^{2+}]_i$ was measured in Ca^{2+}-free media and the cells were treated with thapsigargin (5 μM). After 5 min, thapsigargin was washed out, 1.8 mM calcium was added to the bathing media and $[Ca^{2+}]_i$ was measured for another 5 minutes. A representative trace is shown for each condition. Similar results were obtained for n= 8-10 cells each condition. MG-132 was present in treated cultures throughout the experiment.

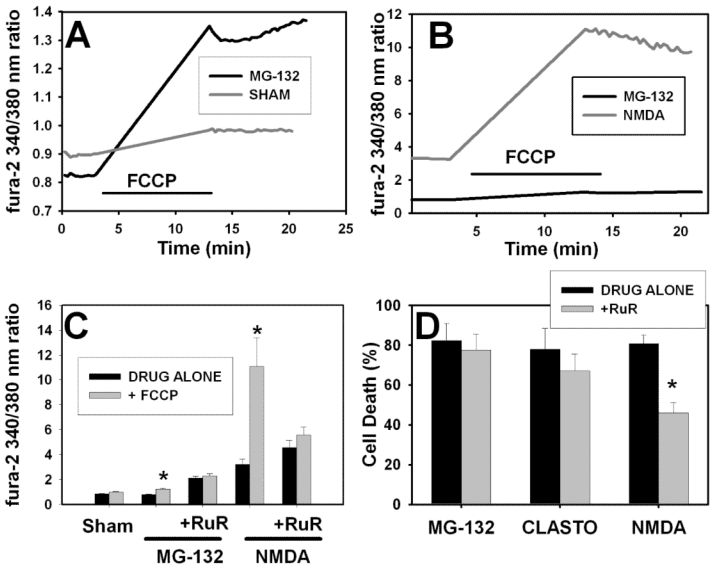

Figure 6. Effects of proteasome inhibitor on mitochondrial Ca^{2+} levels and role of mitochondrial Ca^{2+} in proteasome inhibitor and NMDA-induced neuronal death

A. Murine neocortical cultures were sham-washed (gray line) or treated with MG-132 (1 μM, black line) as in Figure 1. After 3 hr drug treatment, cultures were loaded with fura-2; MG-132 was included in the loading and washing buffers for treated cultures. Cultures were washed into Ca^{2+}-free buffer and basal ratios were obtained. Cultures were treated with FCCP (10 uM) for 10 min, then FCCP was washed out and image acquisition continued. A representative tracing is shown for each condition. Similar results were obtained for at least 40 individual cells per condition in three independent experiments (averaged data is shown in Panel C). B. Cultures were treated with NMDA (300 μM for 10 min, gray line) prior to imaging. Results for NMDA were obtained from n =10 cells in two separate experiments. Data shown here for MG-132 (black line) is same as shown in Panel A; it is reproduced here to demonstrate difference in scale. C. Pooled results for experiments shown in A-B and effect of blockade of the mitochondrial uniporter with ruthenium red. Cultures were treated with NMDA and MG-132 as in A and B. The indicated cultures were pretreated with ruthenium red (RuR, 10 μM) for 1 hr prior to the start of the MG-132 treatment; ruthenium red was present in the indicated cultures throughout the experiment. For NMDA treatment regimen: RuR was added 45 min before NMDA treatment; 300 μM NMDA was added to the cultures for 10 min before the buffers were changed to Ca^{2+} free media; all images were acquired in the Ca^{2+} free media. Values shown are average ± SEM basal 340/380 excitation ratio (time point just prior to addition of FCCP) and peak 340/380 excitation ratio at the end of the 10 min FCCP treatment for at least 40 cells per condition. * indicates "+FCCP" condition differs significantly (P<0.05) from "DRUG ALONE." Differences between basal and peak levels after FCCP were analyzed for significance using Student's t-test. There was no difference between + and − FCCP conditions in cultures treated with ruthenium red. D. Effect of ruthenium red on neuronal death caused by proteasome inhibitors or NMDA. Murine neocortical neurons were treated with 1 μM MG-132 or 10 μM clastolactacystin for 48 hr or with 15 μM NMDA for 24 hr. Ruthenium red was present during the treatment period in the indicated cultures (+RuR, 10 μM). Values shown are mean ± SEM cell death measured using propidium iodide staining at the end of the treatment period. Similar results were obtained using lactate dehydrogenase efflux as a measure of cell death. * indicates "+

RuR" condition differs significantly from "DRUG ALONE" ($P<0.05$ by ANOVA with Bonferroni post hoc).

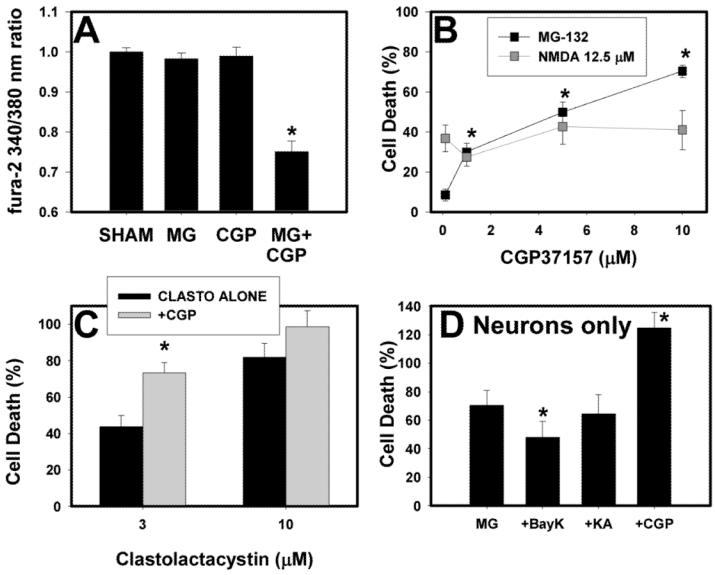

Figure 7. Blockade of mitochondrial Ca^{2+} efflux exacerbates the proteasome inhibitor induced reduction in $[Ca^{2+}]_i$ and neuronal death

A. Murine neocortical cultures were sham-washed (Sham) or treated with 0.3 μM MG-132, 10 μM CGP-37157 (CGP), or both. $[Ca^{2+}]_i$ was measured after 4 hr as in Figure 1. Values shown are mean ± SEM 340/380 ratio for 22-37 cells per condition. * indicates significant difference (P<0.001) from sham condition. B. Cultures were treated with MG-132 (0.3 μM) or NMDA (12.5 μM) alone or with the indicated concentration of CGP-37157; values shown are mean ± SEM cell death as measured by propidium iodide efflux at the end of the treatment period (48 hr for MG-132, 24 hr for NMDA). * indicates that neuronal death in cultures treated with MG-132 + the indicated concentration of CGP-37157 differed significantly from that in cultures treated with MG-132 without CGP-37157 (P<0.05 by ANOVA with Bonferroni post hoc). None of the NMDA+CGP-37157 conditions differed significantly from NMDA alone. Similar results were obtained using lactate dehydrogenase efflux as a measure of neuronal death. C. Cultures were treated with the indicated concentration of clastolactacystin for 48 hr alone or with 10 μM CGP-37157. Values shown are mean ± SEM cell death as measured by propidium iodide efflux; * indicates values in +CGP condition differ significantly from those in clastolactacystin only condition. D. Neuronally-enriched neocortical cultures (>95% neurons) were treated with 0.1 μM MG-132 for 48 hr alone, or in the presence of 10 μM BayK, kainate (KA) or CGP-37157 (CGP). Values shown are mean ± SEM cell death measured by propidium iodide fluorescence at the end of the treatment period. * indicates significant difference (P<0.05 by ANOVA with Bonferroni post hoc) from MG only condition.